Mechanical and Adhesional Manipulation Technique for Micro-assembly under SEM

S. Saito, K. Takahashi and T. Onzawa

Abstract

In recent years, techniques for micro-assembly with high repeatability under a scanning electron microscope (SEM) are required to construct highly functional micro-devices. Adhesion phenomenon is more significant for smaller objects, because adhesional force is proportional to size of the objects while gravitational force is proportional to the third power of it. It is also known that adhesional force between micro-objects exposed to Electron Beam irradiation of SEM increases with the elapsed time. Therefore, mechanical manipulation techniques using a needle-shaped tool by adhesional force are often adopted in basic researches where micro-objects are studied. These techniques, however, have not yet achieved the desired repeatability because many of these could not have been supported theoretically. Some techniques even need the process of trial-and-error. Thus, in this paper, mechanical and adhesional micro-manipulation are analyzed theoretically by introducing new physical factors, such as adhesional force and rolling-resistance, into the kinematic system consisting of a sphere, a needle-shaped tool, and a substrate. Through this analysis, they are revealed that how the micro-sphere behavior depends on the given conditions, and that it is possible to cause the fracture of the desired contact interfaces selectively by controlling the force direction in which the tool-tip loads to the sphere. Based on the acquired knowledge, a mode diagram, which indicates the micro-sphere behavior for the given conditions, is designed. By referring to this mode diagram, the practical technique of the pick and place manipulation of a micro-sphere under an SEM by the selective interface fracture is proposed.

Key Words : Mechanical and adhesional manipulation, SEM, Micro-sphere, Micro-assembly.

1. Introduction

There is a great demand for the technique of micro-object operation in recent years. The technique is expected to be applied to the industrial fields and the basic research fields [1,2]. Adhesive force is dominant compared to gravity in the micro world. Therefore, a gripper does not work properly for a micrometer-sized object, as it does for a millimeter-sized object [3,4]. Although operations based on adhesion with a needle-shaped tool are supposed to be effective for operating a micro-object, it is very difficult to realize highly repeatable operation. For such repeatability, kinematics of a micro-object with the view point of the operation method has been investigated by some groups [5]. These, however, still do not answer the basic question, "Why can a picked object be placed again by only a single needle-shaped tool?" Therefore, in this paper, we analyze micro-object phenomenon caused by the mechanical method using the adhesive effect under the specified condition, and propose pick and place operation of a micro-object based on the analysis. In the following, it should be assumed that we use an SEM as an effective observation device for a micrometer-sized object, and that we operate a micro-object using adhesive force between a micro-object and a needle-shaped tool. To simplify the analysis, we limit the shape of a micro-object to a sphere.

S. Saito, K. Takahashi and *T. Onzawa* : Department of International Development Engineering, Tokyo Institute of Technology, Tokyo Japan
E-mail : saitos@ide.titech.ac.jp

2. Mechanical and adhesional micro-manipulation under SEM

2.1 Micro-sphere adhesional force and rolling-resistance

Micro-objects tend to adhere to other objects because of the size effect. In addition, influence of electron-beam (EB) irradiation should be considered for micro-object adhesion under an SEM. We measured adhesive force of a polystyrene sphere with $2.0\mu m$ diameter [6,7]. In Ref. 7, we clarified the following properties of a micro-object

in EB irradiation.

- Adhesive force increases according to the EB irradiation time after the contact interface is formed.
- The increment rate of adhesive force depends on the EB current.
- Adhesive force initiated by the EB irradiation increases irreversibly even after the irradiation is suspended.

A micro-object is less likely to roll than a macro-object. Due to adhesion, the micro-sphere forms a contact interface having a finite area at the point of contact. This area becomes non-negligible as the size of the sphere decreases. Since the stress distribution in the near field of the contact-interface edge is similar to that in the near field at a crack tip, micro-sphere detachment can be treated as a special case of crack propagation. It is generally known that stress above a certain threshold is required to cause crack propagation [8]. This suggests that detachment of a micro-sphere also requires stress above a certain threshold at the contact-interface edge and thus an external moment greater than a certain threshold must be applied to cause a micro-sphere rolling. This detachment threshold determines the *maximum rolling-resistance* of the micro-sphere. Therefore, we evaluated rolling-resistance using a micro-sphere and a needle-shaped tool with a micro-manipulation system (HMI, Nanorobot II) under a field-emission SEM (Hitachi, S-4200). A scheme of the evaluation method is illustrated in Fig. 1. We used a polystyrene sphere with 2.0μm diameter as a micro-sphere, a tapered glass needle coated with an Au sputtered layer as a tool, and a glass plate coated with an Au sputtered layer as a substrate. The acceleration voltage was 10kV. The magnification ratio was 20000. The procedure was that (i) the tool contacts with the micro-sphere on the side, (ii) the tool loads to the micro-sphere in the lateral direction, and (iii) the tool-tip displacement, δ, is measured at the detachment of the micro-sphere from the substrate due to the tool loading. We calculated actually loaded force, F_{load}, from the measured displacement δ and the lateral tool stiffness, K_{tool}. We obtained the stiffness as K_{tool}=0.50 N/m based on the strength of materials.

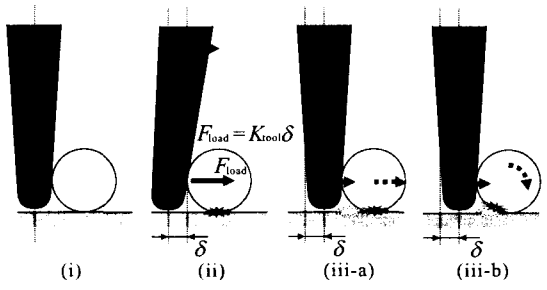

Fig. 1 Schematic illustration of evaluation method of adhesive force and rolling-resistance

By this evaluation method, it was impossible to discriminate between (iii-a) detachment due to slipping and (iii-b) detachment due to rolling since we detected the detachment of a micro-sphere based on the SEM-image observation. Therefore, acquired F_{load} is not directly evaluated rolling-resistance but regarded as min {(*maximum rolling-resistance/radius*), (*maximum friction*)}. We understand the acquired data can be considered the evaluated maximum rolling-resistance of a micro-sphere in the lower limit. The measured F_{load} indicated that the maximum rolling-resistance of at least $0.1\sim 0.2\times10^{-12}$Nm exists even without the EB irradiation.

2.2 Kinematics of mechanical micro-manipulation

A critical state in case of pick and place operation are shown in Fig. 2. In this state, contact interfaces of a micro-sphere are formed with both a tool-tip and a substrate simultaneously. It should be noted that pick and place operation is executed by exchange of contact interfaces before and after this state. Thus, we indicate that it is possible to fracture the contact interface on the desired side selectively by controlling the tool-loading direction to a micro-sphere and induce the condition for the fracture on the desired side.

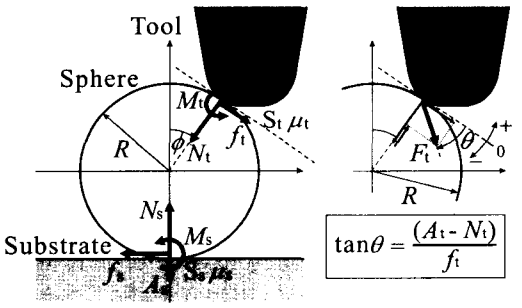

Fig. 2 Critical state of the system

As expressed in Fig. 2, R is a sphere radius of the target system. ϕ is a contact angle. S_s is a contact interface between a sphere and a substrate. S_t is that between a sphere and a tool-tip. A_s, A_t, M_s, M_t, N_s, N_t, f_s, f_t, and μ_s, μ_t are adhesive forces, rolling-resistances, normal forces, frictions, and maximum friction coefficients on S_s and S_t, respectively. It is assumed that the center of the sphere, the contact-point and the center of the tool curvature are on the same straight line. On the assumption of quasi-static process, we obtained the following equilibrium equations.

$$\begin{aligned} 0 &= N_s - A_s + A_t\cos\phi - f_t\sin\phi - N_t\cos\phi \\ 0 &= N_t\sin\phi - A_t\sin\phi - f_t\cos\phi + f_s \\ 0 &= R(f_s + f_t) + M_s + M_t \end{aligned} \quad (1)$$

A loaded force from a tool to a sphere consists of an adhesive force, A_t, a friction, f_t, and a normal force, N_t. When an angle of the force to the tangent is defined as θ ($|\theta| \leq 90$deg), it is expressed by $\tan\theta = (A_t - N_t)/f_t$.

Based on Johnson-Kendall-Roberts (JKR) theory, adhesive forces, A_s and A_t, as adhesion factors are expressed by

$$A_s = \frac{3}{2}\pi\Delta\gamma_s R, \quad A_t = \frac{3}{2}\pi\Delta\gamma_t R' \quad (2)$$

where $\Delta\gamma_s$ and $\Delta\gamma_t$ are works of adhesion on S_s and S_t, respectively. The phenomenon of increasing adhesive force due to the EB irradiation is expressed by the increment of $\Delta\gamma_s$ and $\Delta\gamma_t$. R' in equation (2) is a equivalent radius considering a tool-tip radius of curvature r. This is obtained by $1/R' = 1/R + 1/r$. In this paper, $R' = 0.2R$ is assumed in the case of $r = 0.25R$. We define a *maximum rolling-resistance* on each contact interface as (*constant*) × (*work of adhesion*) × (*contact radius*) with reference to Soltani's work [9]. Concretely, the maximum rolling-resistances are obtained as

$$M_{s\max} = c_r\Delta\gamma_s a_s, \quad M_{t\max} = c_r\Delta\gamma_t a_t \quad (3)$$

where c_r is a maximum rolling-resistance coefficient, and a_s and a_t are contact radiuses on S_s and S_t, respectively. Here, c_r is treated as a constant. It is assumed that the history of EB irradiation influences the magnitude of $\Delta\gamma_s$ and $\Delta\gamma_t$. Since an elastic deformation of a contact interface determines a contact radius, a_s and a_t are obtained by Hertz's relation [10], i.e. $a_s = (R/K)^{\frac{1}{3}} N_s^{\frac{1}{3}}$ and $a_t = (R'/K)^{\frac{1}{3}} N_t^{\frac{1}{3}}$. K is a equivalent elastic modulus which is obtained by $1/K = (3/4)\{(1-\nu_1^2)/E_1 + (1-\nu_2^2)/E_2\}$. E_1 and ν_1 are Young's modulus and Poisson's ratio of the tool and the substrate, respectively. E_2 and ν_2 are those of the sphere.

When a tool loads to a micro-sphere, conditions for causing the slipping on the contact interfaces, S_s and S_t, are expressed by $f_s > \mu_s N_s$ and $f_t > \mu_t N_t$, respectively [11]. By substituting equation (1) into these inequalities,
considering $\tan\theta = (A_t - N_t)/f_t = (A_t - N_t)/(F_t\cos\theta)$, and rearranging them in terms of F_t, we obtain the inequalities written as

$$\begin{aligned} F_t &> \frac{\mu_s A_s}{\mu_s\sin(\theta-\phi) + \cos(\theta-\phi)} (\equiv F_{CS}), \\ F_t &> \frac{\mu_t A_t}{\mu_t\sin\theta + \cos} (\equiv F_{CT}), \end{aligned} \quad (4)$$

where the each right side of inequality (4) is defined as F_{cs} or F_{ct}. Conditional inequality (4) indicate that the slipping on the corresponding interface is caused if the tool-loading force, F_t, increases over a critical force, F_{cs} or F_{cs}, determined by the specified tool-loading angle, θ.

When a tool loads to a micro-sphere, a condition for causing the micro-sphere rolling is that a rolling-resistance generated on each contact interface exceeds the maximum rolling-resistance on the interface. Assuming a maximum rolling-resistance is proportional to the contact radius, it is also naturally assumed that a rolling-resistance is also proportional to the contact radius. Thus, by considering equation (1), we obtain the rolling-resistances written as $M_s = -a_s R(f_s + f_t)/(a_s + a_t)$ and $M_t = -a_t R(f_s + f_t)/(a_s + a_t)$.

Since a condition for micro-sphere rolling is both $|M_s| > M_{s\max}$ and $|M_t| > M_{t\max}$, by considering equation s (1), (2), (3), and $F_t = (f_t/\cos\theta)$, the condition is expressed by

$$\begin{aligned} &RF_t\{\cos(\theta-\phi) + \cos(\theta)\} > c_r \min\{\Delta\gamma_t, \Delta\gamma_s\} \\ &\left[(R/K)^{1/3}\{A_s - F_s\sin(\theta-\phi)\}^{1/3} + (R'/K)^{1/3}(A_s - F_s\sin\theta)^{1/3}\right] \end{aligned} \quad (5)$$

If the left side minus the right side of inequality (5) is defined as $G(F_t)$, $G(F_t) = 0$ has at least one root in the range of $F_t > 0$ because of both $G(0) < 0$ and $G(+\infty) > 0$. If the minimum one of these roots is defined as F_{cr}, the condition for the micro-sphere rolling is written as

$$F_t > F_{cr} \quad (6)$$

Inequality (6) indicates that rolling is caused if a tool-loading force, F_t, increases over the critical force, F_{cr}, determined by the specified tool-loading angle, θ.

2.3 Examination of micro-sphere phenomenon

In this analysis, it is assumed that the material of a tool and a substrate is Au and that of a micro-sphere is polystyrene. The reason for the material assumption is that we can examine the validity of the analysis by referring to the manipulation which we executed in Ref.

1.

Assumed material constants and an assumed contact angle are listed in Table 1. These parameters are used in the following discussion. $\Delta\gamma_{si}$ and $\Delta\gamma_{ti}$ in Table 1 are initial works of adhesion before the EB irradiation on the contact interfaces, S_s and S_t, respectively.

Table 1 List of Parameter of the System

Young's Modulus (Au)	E_1	
Young's Modulus (Polystyrene)	E_2	0.38 [10^4MPA]
Poison's Ratio (Au)	ν_1	0.42 [-]
Poison's Ratio (Polystyrene)	ν_2	0.34 [-]
Maximum Friction Coefficient (S_s)	μ_1	0.8 [-]
Maximum Friction Coefficient (S_t)	μ_2	0.8 [-]
Initial Work of Adhesion (S_s)	$\Delta\gamma_s$	0.1 [N/m]
Initial Work of Adhesion (S_t)	$\Delta\gamma_t$	0.1 [N/m]
Contact Angle	ϕ	30 [deg]

In addition, the maximum rolling-resistance coefficient, c_r, is evaluated in the case of a polystyrene micro-sphere with a 2.0μm diameter ($R=1.0\mu$m). By considering the lower limit of the maximum rolling-resistance, 0.1×10^{-12}Nm , and equation (2) and (3) we obtain the range of the maximum rolling-resistance coefficient as $c_r > c_{rmin} = 2.0\times10^{-5}$m.

Based on the conditions expressed by inequality (4) and (6), the phenomenon can be predicted if a tool loads to a micro-sphere at the tool-loading angle, θ . According to the magnitude of $\min\{F_{cs}, F_{ct}, F_{cr}\}$ for the specified θ, the phenomena can be classified into 3 **Mode** in the following.

Mode S: $F_{cs} = \min\{F_{cs}, F_{ct}, F_{cr}\}$
$\Longleftrightarrow$ Slipping on the substrate-side interface, S_s
Mode T: $F_{ct} = \min\{F_{cs}, F_{ct}, F_{cr}\}$
$\Longleftrightarrow$ Slipping on the tool-tip-side interface, S_t
Mode R: $F_{cr} = \min\{F_{cs}, F_{ct}, F_{cr}\}$
$\Longleftrightarrow$ Rolling of a micro-sphere

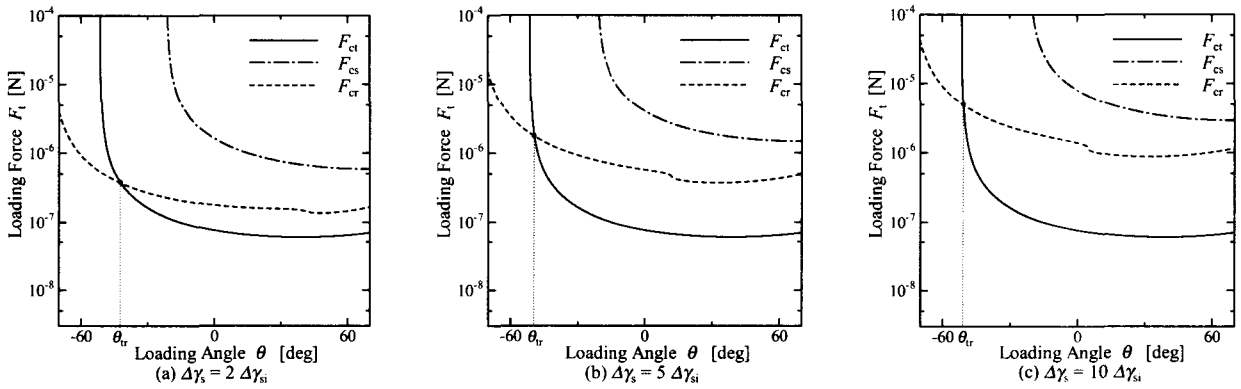

Fig. 3 Critical force F_{cs}, F_{ct}, F_{cr} for θ in case of (a) $\Delta\gamma_s=2\Delta\gamma_{si}$, (b) $\Delta\gamma_s=5\Delta\gamma_{si}$, and (c) $\Delta\gamma_s=10\Delta\gamma_{si}$

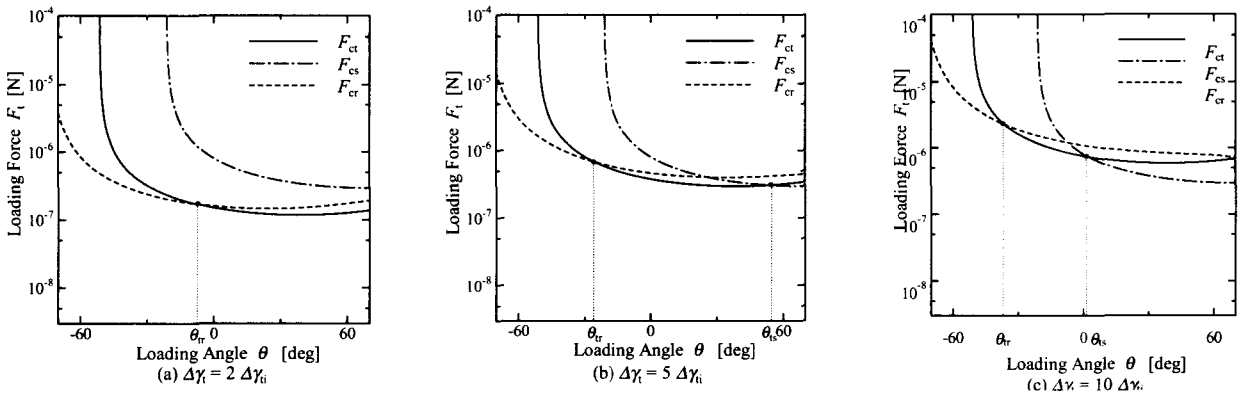

Fig. 4 Critical force F_{cs}, F_{ct}, F_{cr} for θ in case of (a) $\Delta\gamma_t=2\Delta\gamma_{ti}$, (b) $\Delta\gamma_t=5\Delta\gamma_{ti}$, and (c) $\Delta\gamma_t=10\Delta\gamma_{ti}$

Mode S, **Mode T**, and **Mode R** are activated individually. Therefore, by comparing the magnitude of F_{cs}, F_{ct}, and F_{cr} determined by the specified θ, we can examine the micro-sphere phenomenon (**Mode**) caused by a tool.

The influence of the EB irradiation is examined by considering the change of the works of adhesion, $\Delta\gamma_s$ and $\Delta\gamma_t$. In case of pick operation, it is assumed that $\Delta\gamma_s$ increases due to the EB irradiation while $\Delta\gamma_t=\Delta\gamma_{ti}$. To the contrary, in case of place operation, it is assumed that $\Delta\gamma_t$ increases while $\Delta\gamma_s=\Delta\gamma_{si}$.

Fig. 3 shows the relationship between a tool-loading angle, θ, and critical loading forces, F_{cs}, F_{ct}, a nd F_{cr}, in the case that $\Delta\gamma_s$ increases due to the EB irr adiation. (Condition: $\Delta\gamma_t=\Delta\gamma_{ti}, R=1.0\mu\text{m}, c_r=c_{r\min}$)

A critical tool-loading angle, θ_{tr}, determines whether **Mode T** or **Mode R** is caused. Although the value of θ_{tr} is almost the same in any case, the tool-loading force, F_t, for $\theta=\theta_{tr}$ increases in order of (a),(b), and (c). This indicates that a micro-sphere is less likely to roll as $\Delta\gamma_s$ increases due to the EB irradiation although the possible phenomenon (**Mode**) for the specified θ does not change.

Fig. 4 shows the relationship between a tool-loading angle, θ, and critical loading forces, F_{cs}, F_{ct}, and F_{cr}, in the case that $\Delta\gamma_t$ increases due to the EB irradiation. (Condition: $\Delta\gamma_s=\Delta\gamma_{si}, R=1.0\mu\text{m}, c_r=c_{r\min}$)

In the case of (a)$\Delta\gamma_t=2\Delta\gamma_{ti}$, **Mode T** is caused for $\theta>\theta_{tr}$, and **Mode R** is caused for $\theta<\theta_{tr}$ in the same way as shown in Fig. 3. In the case of (b)$\Delta\gamma_t=5\Delta\gamma_{ti}$ and (c)$\Delta\gamma_t=10\Delta\gamma_{ti}$, θ_{tr} determines whether **Mode T** or **Mode R** is caused, and a critical tool-loading angle, θ_{ts}, determines whether **Mode T** or **Mode S** is caused. Therefore, **Mode S** is caused for $\theta>\theta_{ts}$, **Mode T** is caused for $\theta_{ts}<\theta<\theta_{tr}$, and **Mode R** is caused for $\theta<\theta_{tr}$. Both θ_{ts} and θ_{tr} decreases as $\Delta\gamma_t$ increases. Thus, the range of θ for **Mode T**, i.e. $\theta_{tr}\neq\theta_{ts}$, shifts in the negative direction as $\Delta\gamma_t$ increases.

2.4 Mode diagram for micro-sphere phenomenon

From the discussion described above, the possible mic ro sphere phenomenon (**Mode**) for θ can be predicted i f the work of adhesion on the contact interface is specifie d. Fig. 5 shows a mode diagram indicating **Mode** for θ and $(\Delta\gamma_s/\Delta\gamma_t)$. (Condition: $R=1.0\mu\text{m}, c_r=c_{r\min}$)

The abscissa in Fig. 5 should be annotated. In case of $(\Delta\gamma_s/\Delta\gamma_t)>1.0$, $(\Delta\gamma_s/\Delta\gamma_t)=(\Delta\gamma_s/\Delta\gamma_{ti})$, i.e. $\Delta\gamma_s$ increases while $\Delta\gamma_t$ is kept the initial value. In case of $(\Delta\gamma_s/\Delta\gamma_t)<1.0$, $(\Delta\gamma_s/\Delta\gamma_t)=(\Delta\gamma_{si}/\Delta\gamma_t)$, i.e. $\Delta\gamma_t$ increases while $\Delta\gamma_s$ is kept the initial value. To give an example, point A in Fig. 5 indicates Mode S is caused for $\theta=20\,\text{deg}$ in case of $(\Delta\gamma_s/\Delta\gamma_t)=0.1$, i.e. $\Delta\gamma_s=\Delta\gamma_{si}$ and $\Delta\gamma_t=10\Delta\gamma_t$. Conversely, based on this mode diagram, it is possible to control the micro-sphere phenomenon by determining θ if $(\Delta\gamma_s/\Delta\gamma_t)$ is specified as the condition.

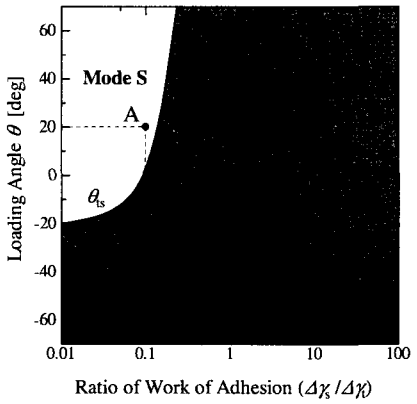

Fig. 5 Mode diagram for phenomenon caused by tool loading

3. Pick and place under SEM by the fracture of micro-sphere interface

In case of pick operation by a needle-shaped tool under an SEM, the main problem is that the f ormer methods do not have repeatability. This is consider ed mainly due to the EB irradiation. A micro-sphere on a substrate is inevitably exposed to the EB bef ore pick operation. Thus, $\Delta\gamma_s$ surely becomes several ti mes as much as $\Delta\gamma_{si}$.

Fig. 6 shows the proposed pick strategy by the selective fracture of the substrate-side interface, S_s, for the reasonably specified θ. This fracture reduces $\Delta\gamma_s$ to less than Δa_{si}. Therefore, this method enables a reasonable pick operation with high repeatability. From this point of view, the empirically effective pick operation described in Ref. 1 and Ref. 7 is considered the method consequently fracturing S_s. Micro-sphere rolling (**Mode R**) should be caused to fracture S_s in case of $(\Delta\gamma_s/\Delta\gamma_t)>1.0$. **Mode R** requires $\theta<\theta_{tr}$ according to Fig. 5. Pick is realized by pulling up a needle-shaped tool immediately after the fracture of S_s. Concretely, point C in Fig. 5 indicates that pick operation is possible by causing **Mode R** for $\theta=-60\,\text{deg}$ even in case of $(\Delta\gamma_s/\Delta\gamma_t)=10$, i.e. $\Delta\gamma_t=\Delta\gamma_{ti}$ and $\Delta\gamma_s=10\Delta\gamma_{si}$.

$\theta<\theta_{tr}$ satisfies the condition for **Mode R** without depending on $\Delta\gamma_s$. However, F_{cr} increases drastically as θ decreases in the range of $\theta<\theta_{tr}$. Thus, too small θ should be avoided in order not to load to an object excessively.

In case of place operation by a needle-shaped tool

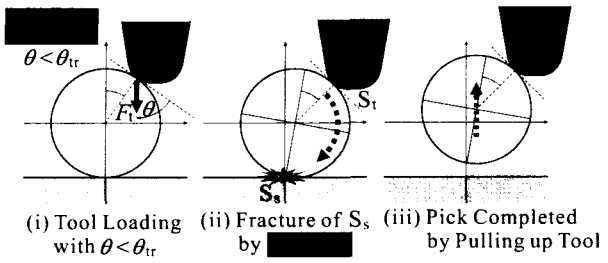

Fig. 6 Pick by the fracture of S_s

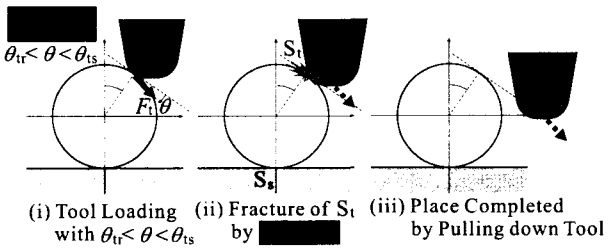

Fig. 7 Place by the fracture of S_t

under an SEM, the main problem is that a micro-sphere often can not be detached from a tool due to large adhesive force on the tooltip-side interface, S_t. This is also due to the EB irradiation. $\Delta\gamma_t$ surely becomes several times as much as $\Delta\gamma_{ti}$, since a micro-sphere adhering to a tool-tip is exposed to the EB before place operation. Fig. 7 shows the proposed place strategy by the selective fracture of S_t for the reasonably specified θ. This method enables a reasonable place operation with high repeatability. From this point of view, the empirically effective place operation described in our papers 1, 8 is considered the method consequently fracturing S_t.

Slipping on S_t (**Mode T**) should be caused to fracture S_t in case of $(\Delta\gamma_s/\Delta\gamma_t)<1.0$. **Mode T** requires $\theta_{tr}<\theta<\theta_{ts}$ according to Fig. 5. Place is realized by pulling down a needle-shaped tool at θ even after the fracture of S_t. Concretely, point B in Fig. 5 indicates that place operation is possible by causing **Mode T** for $theta=-20$deg even in case of $(\Delta\gamma_s/\Delta\gamma_t)=0.1$, i.e. $\Delta\gamma_s=\Delta\gamma_{si}$ and $\Delta\gamma_t=10\Delta\gamma_{ti}$. The range of θ for **Mode T**, $\theta_{tr}\neq\theta_{ts}$, shifts in the negative direction as $\Delta\gamma_t$ increases. Therefore, a tool-loading angle, θ, should be specified cautiously by considering the history of the EB irradiation.

4. Conclusion

In this paper, we analyzed the kinematics of micro-object manipulations and examined practical manipulations under specified conditions. For the analysis, we evaluated rolling-resistance of a $2.0\mu m$-sized polystyrene sphere under an SEM experimentally. This evaluation proved that a maximum rolling-resistance of a micro-sphere exists, and provided the range of the maximum rolling-resistance coefficient. This confirms our theoretical expectation that micro-sphere rolling requires moment above a certain threshold. By considering the evaluation, we constructed a kinematic model of a micro-object manipulation. In addition, we clarified that, even if the adhesive force changes due to the EB irradiation, it is possible to control the micro-sphere phenomenon (Mode) and to fracture the contact interface selectively by tool-loading at the reasonably specified angle. Furthermore, we designed a mode diagram indicating Mode and proposed the best method of pick and place operation based on the mode diagram. From the above knowledge, we first quantitatively understood the mechanical method of a micro-object operation and obtained a guiding principle to the reasonable operation. In the future, it will be important to broaden the knowledge of micro-object operation and to verify that the proposed method is effective through the experiments using a micro-manipulation system.

References

1. H. Miyazaki and T. Sato : Mechanical Assembly of Three-dimensional Microstructures from Fine Particles, *Adv. Robotics*, Vol. 11, No .2 (1997), pp. 169-186
2. H. T. Miyazaki, K. Ohtaka and T. Sato : Photonic Band in Two-dimensional Lattices of Micrometer-sized Spheres Mechanically Arranged under a Scanning Electron Microscope, *Journal of Applied Physics*, Vol. 87, No. 10 (2000), pp. 7152-7158
3. R. S. Fearing : Human Robot Interaction and Cooperative Robots, *Proc. IEEE MEMS*, Vol. 2, Aug (1995), pp. 212-217
4. F. Arai, D. Andou and T. Fulcuda : Micro Manipulation Based on Physical Phenomena in Micro World, *Journal of JSME (C)*, Vol. 62, No. 603 (1996), pp. 4286-4293 (in Japanese)
5. M. Sitti and H. Hashimoto : Controlled Pushing of Nanopaticles : Modeling and Experimensts, *IEEE/ASME Trans. Mechatronics*, Vol. 5, No. 2 (2000), pp. 199-211
6. H. T. Miyazaki, Y. Tomizawa, K. Koyano, T. Sato and N. Shinya : Adhesion Force Measurement System for Micro-objects in a Scanning Electron Microscope, *Rev. Sci. Inst.*, Vol. 71, No. 8 (2000), pp. 3123-3131
7. H. T. Miyazaki, Y. Tomizawa, S. Saito, T. Sato and N. Shinya : Adhesion of Micrometer-sized Polymer Particles under a Scanning Electron Microscope, *Journal of Applied Physics*, Vol. 88, No. 6 (2000), pp.

3330-3340
8. H. Kobayashi : Fracture Mechanics, *Kyouritu Press*, (1993) (in Japanese)
9. M. Soltani and G. Ahmadi : On Particle Removal Mechanisms under Base Acceleration, *Journal of Adhesion*, Vol. 44, (1994), pp. 161-175
10. S. Timoshenko et al. : Theory of Elasticity 3rd edn., *McGraw-Hill. Inc.*, (1951)
11. Y. Ando, Y. Ishikawa and T. Kitahara : Friction Characteristic and Adhesion Force under Low Normal Load, *Trans. ASME J. Tribology*, Vol. 117, No. 4 (1995), pp. 569-574